

# Scaling and super-universality in the coarsening dynamics of the $3d$ random field Ising model

**Camille Aron**

Université Pierre et Marie Curie - Paris VI, Laboratoire de Physique Théorique et Hautes Énergies, 4 Place Jussieu, 75252 Paris Cedex 05 France

**Claudio Chamon**

Physics Department, Boston University, Boston, MA 02215, USA

**Leticia F. Cugliandolo and Marco Picco**

Université Pierre et Marie Curie - Paris VI, Laboratoire de Physique Théorique et Hautes Énergies, 4 Place Jussieu, 75252 Paris Cedex 05 France

**Abstract.** We study the coarsening dynamics of the three-dimensional random field Ising model using Monte Carlo numerical simulations. We test the dynamic scaling and super-scaling properties of global and local two-time observables. We treat in parallel the three-dimensional Edward-Anderson spin-glass and we recall results on Lennard-Jones mixtures and colloidal suspensions to highlight the common and different out of equilibrium properties of these glassy systems.

## 1. Introduction

The physics of domain growth is well understood [1, 2]. Just after the initial thermal quench into the ordered phase, the spins in a ferromagnetic system tend to order and form domains of the equilibrium states. In clean systems the ordering dynamics is governed by the symmetry and conservation properties of the order parameter. When impurities are present the dynamics are naturally slowed down by domain-wall pinning [3]. The dynamic scaling hypothesis states that the time-dependence in any macroscopic observable enters only through a growing length scale,  $R(t)$ , either the instantaneous *averaged* or *typical* domain radius. However, a complete description of the phenomenon is lacking. In the pure cases the scaling functions are not known analytically and no fully satisfactory approximation scheme to estimate them is known [1]. In presence of disorder the limitations are more severe in the sense that the growth laws are derived by assuming that the relaxation is driven by activation over free-energy barriers and the properties of the latter are estimated with energy balancing arguments applied to single interfaces that are hard to put to the test. Even in the relatively simple

random bond Ising model (RBIM) the time dependence of the growth law remains a subject of controversy [4].

Quenched randomness may be weak or strong in the sense that the first type does not change the nature of the low-temperature phase, as in the random bond or random field Ising (RFIM) models, or it can change it as in spin-glasses. Fisher and Huse conjectured that in the first class of systems, once the scaling hypothesis is used to describe the long times dynamics, so that times and lengths are measured in units of  $R(t)$ , no out of equilibrium observable depends on the quenched randomness [5] and their scaling functions are thus identical to the ones of the pure limit. This is the so-called ‘*super-universality*’ hypothesis in coarsening phenomena. Tests of this hypothesis as applied to the equal-times two-point function of the 3d RFIM and the 2d RBIM appeared in [6] and [7], respectively, and the distribution of domain areas in the 2d RBIM in [8].

The dynamics of generic glassy systems is less well understood but presents some similar aspects to those mentioned above. The droplet model of finite-dimensional spin-glasses is based on the assumption that in the low-temperature phase these systems also undergo domain growth of two competing equilibrium states [5]. In the mean-field limit spin-glasses have, though, a very different kind of dynamics [9, 10] that cannot be associated to a simple growth of two types of domains. Numerical studies of the 3d Edwards-Anderson (EA) model [11, 12, 13, 14, 15] have not been conclusive in deciding for one or the other type of evolution and, in a sense, show aspects of both. A one-time dependent ‘coherence’-length,  $R(t)$ , has been extracted from the distance and time dependence of the *equal-time* overlap between two replicas evolving independently with the same quenched disordered interactions [12, 13, 15]. A power-law  $R(t) \sim t^{1/z(T)}$  with the dynamic exponent  $z(t) = z(T_c)T_c/T$  fits the available data for the 3d EA and  $z(T_c) = 6.86(16)$  with Gaussian [15] and  $z(T_c) = 6.54(20)$  with bimodal [12, 13] couplings. Still, it was claimed in [15] that the overlap decays to zero as a power law at long distances and long times such that  $r/R(t)$  is fixed, implying that there are more than two types of growing domains in the low temperature phase.

A two-time dependent length,  $\xi(t, t_w)$ , can be extracted from the analysis of the spatial decay of the correlation between two spins in the same system at distance  $r$  and different times  $t$  and  $t_w$  after preparation [16]. The latter method is somehow more powerful than the former one in the sense that it can be easily applied to glassy problems without quenched disorder. If there is only one characteristic length-scale in the dynamics  $R(t)$  should be recovered as a limit of  $\xi(t, t_w)$  but this fact has not been demonstrated.

The mechanism leading to the slow relaxation of structural glasses is also not understood. Still, molecular dynamic studies of Lennard-Jones mixtures [17] and the analysis of confocal microscopy data in colloidal suspensions [18] show that two-time observables have similar time dependence as in the 3d EA model. Two-time correlations scale using ratios of one-time growing functions that, however, cannot be associated to a domain radius yet. A two-time correlation length  $\xi$  with characteristics similar to the

one in the 3d EA can also be defined and measured.

The understanding of dynamic fluctuations in out of equilibrium relaxing systems appears as a clear challenge [19]. In systems with quenched randomness different sample regions feel a different environment and one expects to see their effect manifest in different ways working at fixed randomness. The effect of quenched randomness is at the root of Griffiths singularities in the statics of disordered systems, for instance. In structural or polymer glasses there are no quenched interactions instead, but still one expects to see important fluctuations in their dynamic behaviour both in metastable equilibrium and in the glassy low temperature regime. The question of whether the fluctuations in generic glassy systems resemble those in coarsening systems has only been studied in a few solvable cases such as the model of ferromagnetic coarsening in the large  $N$  limit [20] and the Ising chain [21].

In this paper we study ferromagnetic ordering in the 3d RFIM following a quench from infinite temperature and we compare it to the dynamics of the 3d EA spin-glass and particle glassy systems. Our aim is to signal which aspects of their out of equilibrium evolution differ and which are similar by focusing on freely relaxing observables – no external perturbation is applied to measure linear responses. We test the scaling and super-universality hypothesis in the RFIM and we explicitly show that the latter does not apply to the EA model. We analyse the spatio-temporal fluctuations in the coarsening problem and we compare them to the ones found in spin-glasses [14, 16], the  $O(N)$  ferromagnetic coarsening in the large  $N$  limit [20], and other glassy systems [18, 22, 23].

The organisation of the paper is the following. In Sect. 2 we define the models and we describe the numerical procedure. Section 3 is devoted to the study of the growing length scale,  $R$ , the scaling and super-universality hypothesis, and the two-time growing length,  $\xi$ . In Sect. 4 we focus on the local fluctuations of two time observables. We study two-time coarse-grained correlations and we analyse their statistical properties as time evolves. Finally, in Sect. 5 we present our conclusions.

## 2. The models

Two varieties of quenched disorder are encountered in spin models: randomness in the strength of an externally applied magnetic field and randomness in the strength of the bonds. The RFIM and the EA spin-glass are two archetypal examples of these. In this Section we present their definitions and we recall some of their main properties.

### 2.1. The Random Field Ising Model

The 3d Random Field Ising model (RFIM) is defined by the Hamiltonian [24]

$$H = -J \sum_{\langle i,j \rangle} s_i s_j - \sum_i H_i s_i. \quad (1)$$

The first term encodes short range ferromagnetic ( $J > 0$ ) interactions between nearest neighbour Ising spins,  $s_i = \pm 1$ , placed on the nodes of a cubic lattice with linear size  $L$ .  $H_i$  represents a local random magnetic field on site  $i$ . We adopt a bimodal distribution for these independent identically distributed random variables ( $H_i = \pm H$  with equal probability).  $H$  quantifies the strength of the quenched disorder. Hereafter we set  $J = 1$  and we use units in which  $k_B = 1$ .

The RFIM is relevant to a large class of materials due to the presence of defects that cause random fields. Dilute anisotropic antiferromagnets in a uniform field are the most studied systems expected to be described by the RFIM. Several review articles describe its static and dynamic behaviour [3] and the experimental measurements in random field samples have been summarized in [25]. Dipolar glasses also show aspects of random field systems [26].

In the case  $H = 0$ , the RFIM reduces to the well known clean Ising model with a phase transition from a paramagnetic to a ferromagnetic state occurring at  $T_c \simeq 4.515$ . It is well established that in  $d = 3$  (not in  $d = 2$ ) there is a phase separating line on the  $(T, H)$  plane joining  $(T_c, H = 0)$  and  $(T = 0, H_c)$ . At  $T = 0$  and small magnetic field, it has been rigorously proven that the state is ferromagnetic [27, 28]. The nature of the transition close to zero temperature has been the subject of some debate. Claims of it being first order [29] have now been falsified and a second order phase transition has been proven [30, 31]. It was also argued but not established that there might be a spin-glass phase close to  $(T = 0, H_c)$  [32]. Recent numerical simulations yield  $H_c \simeq 2.215(35)$  at  $T = 0$  [33, 34].

## 2.2. The Edwards-Anderson spin-glass

The 3d Edwards-Anderson (EA) spin glass is defined by

$$H = - \sum_{\langle i,j \rangle} J_{ij} s_i s_j. \quad (2)$$

The interaction strengths  $J_{ij}$  act on nearest neighbours on a cubic three-dimensional lattice and are independent identically distributed random variables. We adopt a bimodal distribution,  $J_{ij} = \pm 1$  with equal probability. This model undergoes a static phase transition from a paramagnetic to a spin-glass phase at  $T_g \simeq 1.14(1)$  [35]. The nature of the low temperature static phase is not clear yet and, as for the out of equilibrium relaxation, two pictures developed around a situation with only two equilibrium states as proposed in the droplet model and a much more complicated vision emerging from the solution of the Sherrington-Kirkpatrick model, its mean-field extension [36].

## 2.3. Numerical methods

We focus here on the out of equilibrium relaxation in the ordered phase. We simulate the dynamics following an instantaneous quench from infinite temperature at the initial

time,  $t = 0$ , by choosing a random initial condition:  $s_i(t = 0) = \pm 1$  with probability one half. The order parameter is not conserved during the evolution. We use the continuous time Monte Carlo (MC) procedure [37, 38, 39]. This algorithm, which is nothing else than a re-organisation of the standard Monte Carlo rule, is rejection free. This makes it spectacularly faster than standard MC which would have a rejection rate close to 1 in the ferromagnetic phase of the RFIM. Times are expressed in usual Monte Carlo steps (MCs): 1 MCs corresponds to  $N = L^d$  spin updates with the standard MC algorithm. The way to translate from the continuous time MC to standard MC units, in which we present our results, is explained in [37, 38, 39].

We study the relaxation dynamics with non-conserved order parameter in the ( $d = 3$ ) ferromagnetic phase of the RFIM at relatively low temperature and small applied field. Interesting times are not too short – to avoid a short transient regime – and not too long – to avoid reaching equilibration (in ferromagnetic coarsening a non-zero magnetization density indicates that the coarsening regime is finished and other more refined methods are used in the spin-glass case [40]). We delay equilibration by taking large systems since the equilibration time rapidly grows with the size of the lattice. A reasonable numerical time-window is  $[10^3, 10^7]$  MCs. We show results obtained using lattices with  $L = 250$  ( $N = 1.5 \times 10^7$  spins) in the RFIM and  $L = 100$  ( $N = 10^6$  spins) in the spin-glass. We checked that finite size effects are not important in any of these cases for averaged quantities.

### 3. The typical growing length

In this Section we study the typical growing length (a geometric object) in the RFIM and the EA model. We establish scaling and super-universality relations for three types of correlations functions (statistical objects). Two of them involve either two space points and one time, or one space point and two times, and are the usual observables studied in coarsening phenomena. The third one is commonly used in the study of glassy systems where two-point correlations are not sufficient to characterize the dynamics of the systems [14, 16, 17, 18] and allows for the definition of a two-time dependent length that we can compare to the one obtained in the 3d EA model and glassy particle systems.

#### 3.1. The RFIM

During the ferromagnetic coarsening regime, there are as many positive as negative spins in such a way that the magnetization density stays zero in the thermodynamic limit and weakly fluctuates around zero for finite size systems. Everywhere in the sample, there is a local competition between growing domains. Eventually, after an equilibration time  $\tau_{eq}$  (that diverges with the system size), one of the two phases conquers the whole system scale.

In the coarsening regime (times shorter than  $\tau_{eq}$ ) dynamic scaling [1] applies and the growth of order is characterized by a *typical domain radius*,  $R(t; T, H)$ , that increases

in time and depends on the control parameters,  $T$  and  $H$ , and the dimension of space,  $d$  [41]. While in the absence of impurities it is clearly established that, for non-conserved order parameter dynamics, the domain length  $R$  grows as  $R \sim t^{1/2}$  independently of  $d$  [1] with a prefactor that monotonically decreases upon increasing temperature [42], the functional form of  $R$  is less clear in random cases. Scaling arguments based on the energetics of single interfaces [3, 43, 44, 45] predict a crossover from the pure case result at short time-scales when it is easy to inflate, to a logarithmic growth,

$$R(t; H, T) = \frac{T}{H^2} \ln(t/\tau(T, H)) . \quad (3)$$

The fact that the prefactor grows with  $T$  (as opposed to what happens for pure curvature driven dynamics [42]) is due to the activated character of the dynamics. Several proposals for the characteristic time  $\tau$  exist:  $\tau \sim (T/H^2)^2$  [43, 2] and  $\tau \sim \tau_0 e^{A(T)/H^2}$  with  $A(T)$  a weakly temperature dependent function [6]. To ease the notation in what follows we do not write explicitly the  $T$  and  $H$  dependence of  $R$ .

From the point of view of the renormalization group, all points within the ferromagnetic region of the  $(T, H)$  phase diagram flow to the stable, zero-temperature, zero-disorder sink. Hence, randomness and temperature should be irrelevant in equilibrium at  $T < T_c$ . The super-universality hypothesis states that for non equilibrium ordering dynamics, once lengths are scaled with the typical length  $R$ , quenched random fields are irrelevant and all scaling functions are the ones of the pure 3d Ising system at  $T = 0$  with non-conserved order parameter.

*3.1.1. The equal-time spatial correlation.* A careful analysis of the field and time dependence of the growing length scale together with tests of the scaling hypothesis applied to the equal-time correlation

$$C_2(r; t) \equiv \langle s_i(t) s_j(t) \rangle_{|\vec{r}_i - \vec{r}_j| = r} , \quad (4)$$

where the average runs over all spins in the sample, appeared in [6, 48]. In the coarsening regime, at distances  $a \ll r \ll L$  with  $a$  the lattice spacing and  $r/R(t)$  finite,  $C_2(r; t)$  is expected to depend on  $r$  and time  $t$  only through the ratio  $r/R$ ,

$$C_2(r; t) \simeq m_{eq}^2 f_2(r/R(t)) , \quad (5)$$

with  $m_{eq}$  the equilibrium magnetization density (that decreases with increasing  $T$  and/or  $H$ ),  $\lim_{x \rightarrow 0} f_2(x) = 1$  and  $\lim_{x \rightarrow \infty} f_2(x) = 0$ . Since the spatial decay is approximately exponential,  $C_2(r; t) \propto e^{-r/R(t)}$  for not too long  $r$ , we use this functional form to extract  $R$  from the data fit at each set of parameters  $(T, H, t)$ . Figure 1 (a) shows that the growing length  $R$  has two regimes: shortly after the quench  $R$  grows as  $t^{1/2}$  like in the pure case and it later crosses over to a logarithmic growth. This is consistent with previous numerical studies in 2d [7, 47] and 3d systems [6, 48]. In Fig. 1 (b) we test the dependence on  $T$  and  $H$  by plotting  $\frac{H^2}{T} R$  versus  $t/\tau$  for  $T = 1, 2$  and  $H = 0.5, 1, 1.5$ . We found the best collapse using  $\tau \sim H^{-3}$  but the precision of our data is not high enough to distinguish between this and the  $\tau$ s proposed in [43] and [6]. Our numerical results tend to confirm the  $T/H^2$  dependence of  $R$  even in the early stages of the growth.

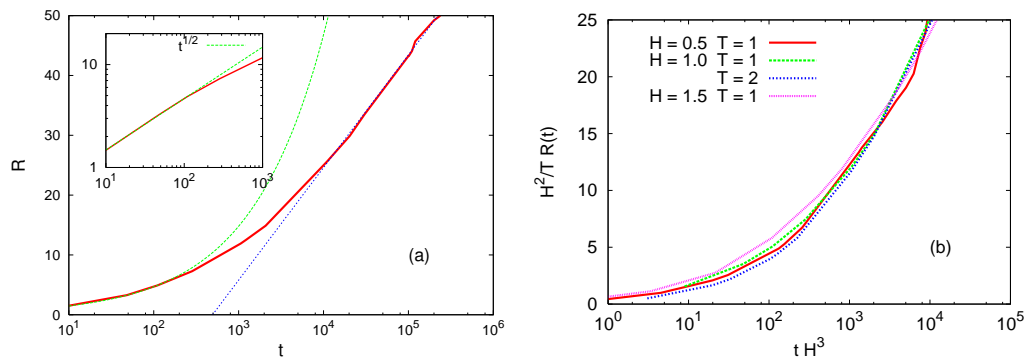


**Figure 1.** (a) With line-points (red), the growing length  $R(t)$  at  $T = 1$  and  $H = 1$ . The green curve is the power law  $\sqrt{t}$  that describes well the data at short times, right after the temperature quench. The blue line is a logarithmic law apt to describe the behaviour at longer time-scales. In the inset: the same data in a log-log scale to highlight the quality of the  $\sqrt{t}$  behaviour at short times. (b) Study of the dependence of  $R$  on the parameters  $T$  and  $H$  for two values of  $T$  and three random field strengths  $H$  given in the key.

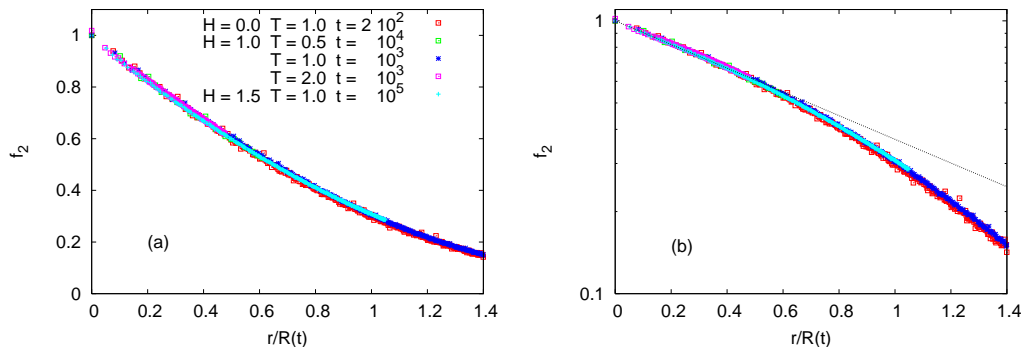


**Figure 2.** (a) The scaling function  $f_2(r/R)$  for  $T = 0.5, 1, 2$  and  $H = 1, 1.5$ . (b) The same data in a linear-log scale showing that  $f_2$  is close to an exponential at short  $r/R$ .

Since the work of [6], it is now clear that  $f_2$  in Eq. (5) is independent of  $H$ , and very similar to the one of the pure system. In Fig. 2 we also find that the scaling functions  $f_2$  at different  $T$  fall on top of one another. Thus  $f_2$  is independent of  $H$  and  $T$ .

*3.1.2. The two-time self-correlation.* It is commonly defined as

$$C(t, t_w) \equiv \frac{1}{N} \sum_{i=1}^N \langle s_i(t) s_i(t_w) \rangle, \quad (6)$$

and quantifies how two spin configurations of the same system, one taken at  $t_w$  (waiting time) and the other one at  $t \geq t_w$ , are close to each other. The angular brackets here indicate an average over different realizations of the thermal noise. In the large  $N$  limit, this quantity is self-averaging with respect to noise and disorder induced fluctuations. This two-time function has been used as a clock for the out of equilibrium dynamics of

glassy systems [9, 10] and we shall use this property again, in the study of the two-time growing length and fluctuations.

The behaviour of  $C$  is well understood for coarsening systems. As long as the domain walls have not significantly moved between  $t_w$  and  $t(> t_w)$  (that defines what we shall call later short time delay), the self-correlation is given by the fluctuations of spins that are in thermal equilibrium inside the domains. As any other equilibrium two-time function, the self-correlation depends then only on  $t - t_w$ . Later, for longer time delays, the displacement of domain walls cannot be neglected any more and  $C$  loses its time-translational invariance. The self-correlation can be written as a sum of two terms representing the thermal and aging regimes:

$$C(t, t_w) = C_{\text{th}}(t - t_w) + C_{\text{ag}}(t, t_w) \quad (7)$$

with the limit conditions

$$\begin{aligned} C_{\text{th}}(0) &= 1 - q_{\text{EA}} , & \lim_{t_w \rightarrow t^-} C_{\text{ag}}(t, t_w) &= q_{\text{EA}} , \\ \lim_{t - t_w \rightarrow \infty} C_{\text{th}}(t - t_w) &= 0 , & \lim_{t \gg t_w} C_{\text{ag}}(t, t_w) &= 0 . \end{aligned}$$

$q_{\text{EA}}$  is a measure of the order parameter and in a ferromagnetic phase it simply equals  $m_{\text{eq}}^2$ , the magnetization squared.

In Fig. 3 (a) we show the decay of the two-time correlation  $C$  as a function of the time delay  $t - t_w$  for  $t_w = 10^3, 10^4, 10^5$  at  $T = 1$  and  $H = 1$ . On each of these curves, one can distinguish the two dynamic regimes. The longer the waiting time the later the aging regime appears. In Fig. 3 (b) we show the decay of the two-time correlation as a function of time-delay for  $t_w = 10^3$  and five pairs of parameters  $(T, H)$  given in the key. It is clear that the full relaxation depends strongly on the external parameters: raising the temperature or reducing the random field strength speeds up the decay. For these values of  $T$  and  $H$ ,  $q_{\text{EA}}$  does not change much but the decay in the aging regime does.

Dynamic scaling implies that in the aging regime

$$C_{\text{ag}}(t, t_w) = q_{\text{EA}} f\left(\frac{R(t)}{R(t_w)}\right) , \quad (8)$$

with  $R$  the typical length extracted from  $C_2$ ,  $f(1) = 1$  and  $f(\infty) = 0$ . For our choice of parameters  $(T, H)$ ,  $q_{\text{EA}}$  is close to unity so we can easily compute  $f$  from the measured  $C$  by using  $f = C_{\text{ag}}/q_{\text{EA}} \simeq C/q_{\text{EA}}$ . Super-universality states that  $f$  does not depend on  $T$  and  $H$ . In Fig. 4 we show that both hypotheses apply to this quantity. In panel (a) we use a linear-linear scale while in panel (b) we present the same data in a double logarithmic scale. Although the scaling function  $f$  looks like a power law it is not. One expects that its tail [ $R(t) \gg R(t_w)$ ] becomes a power-law with an exponent  $\lambda$ . The actual function  $f$  is not known. Most of the analytic efforts in domain growth studies are devoted to develop approximation schemes to derive  $f$ ,  $f_2$  and other scaling functions but none of them is fully successful [1].

*3.1.3. The four point-correlation function.* In order to successfully identify a growing correlation length in glassy systems including the 3d EA spin-glass, one defines the



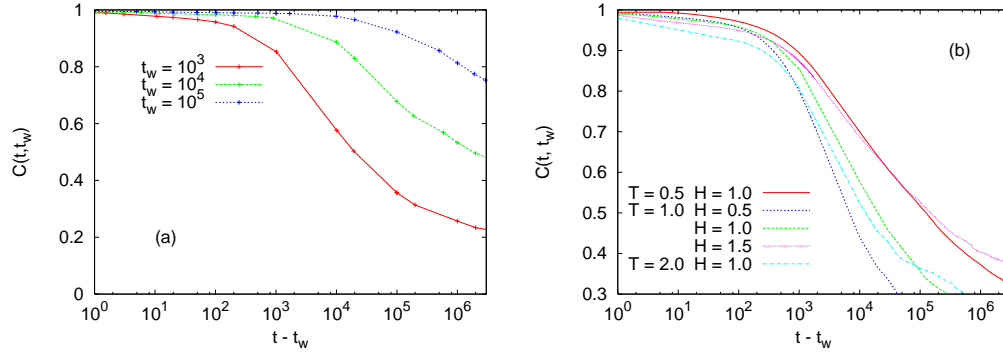


**Figure 3.** The global correlation  $C$  vs  $t - t_w$ . (a)  $T = 1$  and  $H = 1$  and different  $t_w$  given in the key. (b)  $t_w = 10^3$  at various pairs of  $(T, H)$  given in the key.

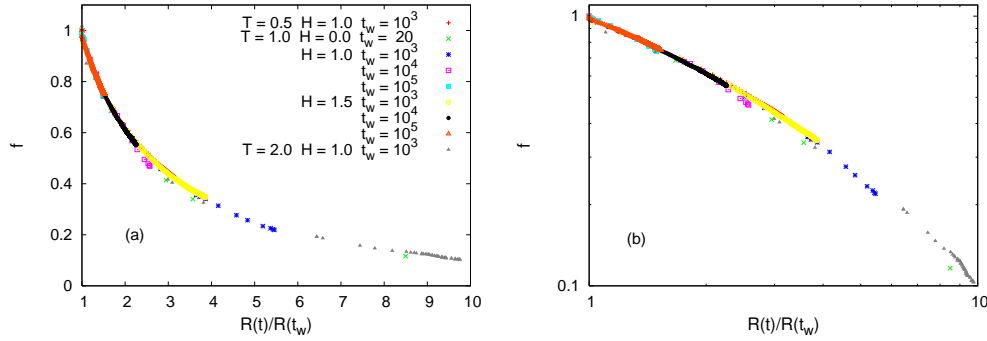


**Figure 4.** Test of the scaling and super-universality hypothesis. (a)  $f = C_{ag}/q_{EA}$  vs.  $R(t)/R(t_w)$  at various pairs of  $(T, H)$  and  $t_w$  given in the key. (b) The same data in log-log scale.

two-time two-site correlation function [14, 16, 17, 18, 49]

$$C_4(r; t, t_w) \equiv \langle s_i(t) s_i(t_w) s_j(t) s_j(t_w) \rangle_{|\vec{r}_i - \vec{r}_j| = r}. \quad (9)$$

We extract  $\xi$  from its approximate spatial exponential decay:  $C_4(r; t, t_w) - C^2(t, t_w) \propto e^{-r/\xi(t, t_w)}$  at relatively short  $r/\xi$ . (Other methods, like defining the connected four spin-correlation and extracting  $\xi$  from its volume integral yield similar qualitative results though slightly different quantitatively.) Results of this analysis are shown in Fig. 5 (a) where we plot  $\xi(t, t_w)$  as a function of  $t$  for different  $t_w$  at  $T = 1$  and  $H = 1$ . We identify a short  $t - t_w$  regime that is independent of  $t_w$  (thermal regime), whereas for long  $t - t_w$ , time-translational invariance is broken (aging regime). In Fig. 5 (b) we plot  $\xi(t, t_w)$  versus  $1 - C(t, t_w)$  for the three same values of  $t_w$ , using  $t$  as a parameter. The dependence on  $1 - C$  and  $t_w$  is monotonic and very similar to the one obtained in the 3d EA model [14] (see Fig. 7). The thermal regime is almost invisible here since it is contained between  $C = 1$  and  $C = q_{EA}$ , with  $q_{EA} \simeq 1$  for this set of parameters. We then propose

$$\xi(t, t_w) = R(t_w) g(C). \quad (10)$$

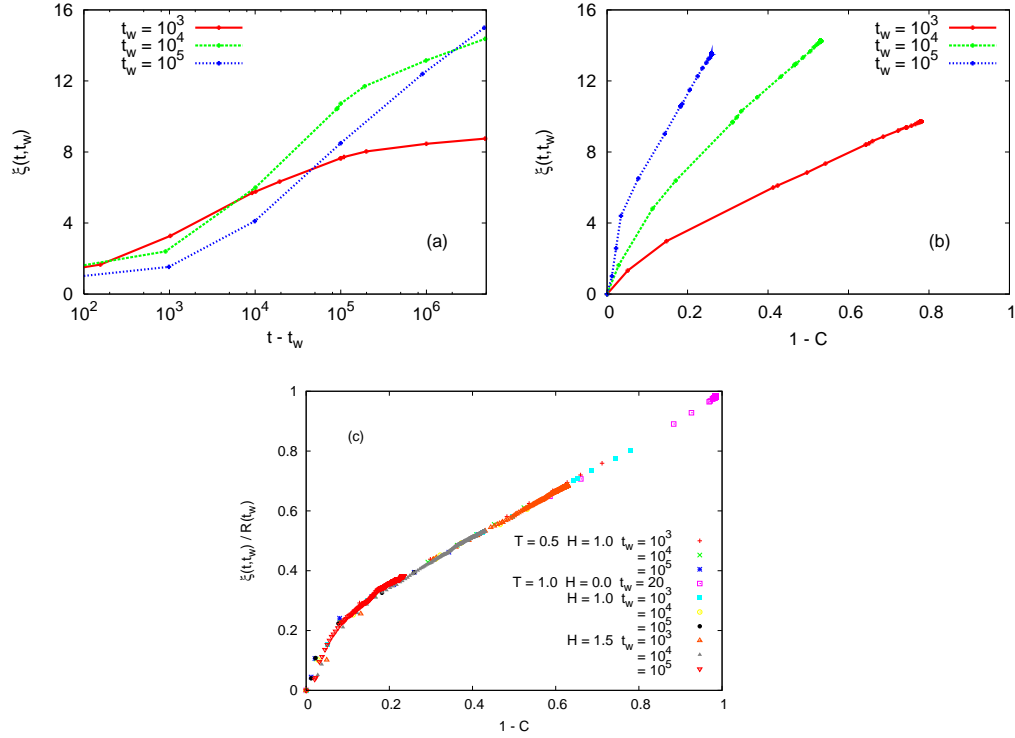


**Figure 5.** The two-time correlation length,  $\xi$ , in the RFIM. (a)  $\xi$  as a function of time-delay,  $t - t_w$  for several values of  $t_w$  given in the key at  $T = 1$  and  $H = 1$ . (b)  $\xi$  as a function of the global correlation in a parametric plot at  $T = 1$  and  $H = 1$ . (c) Scaling  $\xi(t, t_w) = R(t_w) g(C)$  at two temperatures and two values of the random field using three waiting-times  $t_w$  for each set of parameters. The pure case  $H = 0, T = 1$  is also included with a very short  $t_w$  to avoid equilibration.

The limit  $g(C = 1) = 0$  is found by taking  $t = t_w$ , that corresponds to  $C = 1$  [extending the scaling form (10) to include the thermal regime]. In this case  $C_4(r; t, t) = 1$ . If one uses  $C_4(r; t, t) = \tilde{C}_4(r/\xi, C(t, t) = 1)$ , see Sect. 3.1.4, then  $\xi(t, t)$  must vanish to obtain  $C_4$  independent from  $r$ , and this imposes  $g(1) = 0$ . In the other extreme, when  $t \gg t_w$  and  $C = 0$  one expects  $g(0) = 1$ . The reason is the following.  $\lim_{t \gg t_w} C_4(r; t, t_w) = C_2(r, t)C_2(r, t_w)$ , for the temporal decoupling of  $C_4$  can be done in the  $t \gg t_w$  limit. Recalling that  $C_2(r, t) \propto f_2(r/R(t))$  with  $\lim_{x \rightarrow 0} f_2(x) = 1$ , the only spatial contribution to  $\lim_{t \gg t_w} C_4(r; t, t_w)$  comes from the term  $C_2(r, t_w) \propto f_2(r/R(t_w))$ . Using  $\lim_{t \gg t_w} \xi(t, t_w) = R(t_w)g(0)$  and further assuming that the functional forms of  $C_4(x)$  and  $f_2(x)$  are, to a first approximation, the same we deduce  $g(0) = 1$ .

Figure 5 (c), where we plot  $\xi(t, t_w)/R(t_w)$  versus  $1 - C(t, t_w)$  for different  $t_w$ , illustrates the validity of the scaling hypothesis (10). We see that, as expected,  $g(C = 1) = 0$  and it seems plausible that  $\lim_{C \rightarrow 0} g(C) = 1$ . The scaling function  $g$  is found to satisfy super-universality, *i.e.* it is independent of  $H$  and  $T$ .

**3.1.4.  $C_4$  and super-universality.** Using the monotonicity properties of  $C$  as a function of  $t - t_w$  and  $t_w$ , and of  $\xi$  as a function of  $t_w$  and  $1 - C$  we can safely exchange the

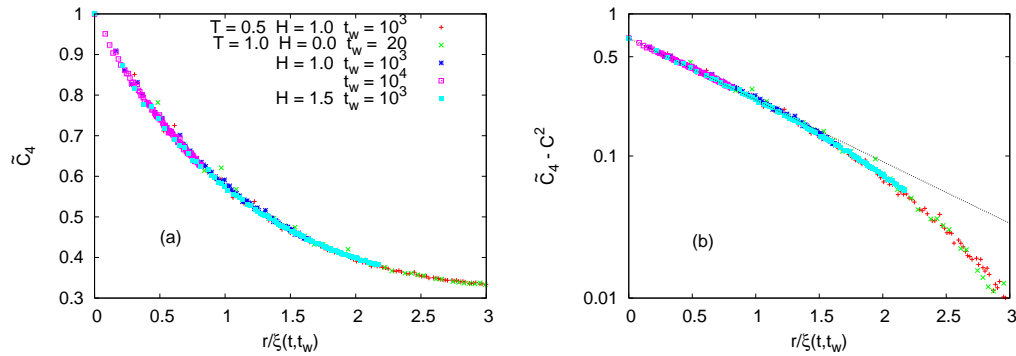


**Figure 6.** (a) Test of scaling,  $\tilde{C}_4(r/\xi, C)$ , and the super-universality of  $\tilde{C}_4$  for the parameters  $T$  and  $H$  given in the key. Times  $t$  and  $t_w$  are chosen in such a way that  $C(t, t_w) = 0.57$  in all cases. (b) The same data in linear-log scale showing that  $\tilde{C}_4 - C^2$  is very close to an exponential at short  $r/\xi$ .

dependence of  $C_4$  on the two times by a dependence on  $\xi$  and  $C$ . In other words,  $C_4(r, \xi, C)$  where, again for simplicity, we did not write explicitly the dependence on  $T$  and  $H$ . Now, a reasonable scaling assumption is that one can measure  $r$  in units of  $\xi$  such that

$$C_4(r, t, t_w) = \tilde{C}_4(r/\xi(t, t_w), C(t, t_w)). \quad (11)$$

In Fig. 6 we put this scaling form to the test and we examine the possible super-universality of  $\tilde{C}_4$ . We use different values of the parameters  $t$ ,  $t_w$ ,  $T$ ,  $H$  such that  $C = 0.57$  in all cases. Both scaling and super-universality relations are well satisfied. Note that the scaling relation in Eq. (11) can also be transformed into

$$C_4(r; t, t_w) = C_4(r/R(t_w), R(t)/R(t_w)) \quad (12)$$

by using Eq. (8). This last scaling form was also found for the  $O(N)$  ferromagnetic model in the large  $N$  limit although the scaling function does not have a simple exponential relaxation [20].

### 3.2. 3d EA

A detailed analysis of the relaxation properties of similar correlations in the 3d EA model appeared in [14]. The spatial one-time correlation,  $C_2(r, t)$ , vanishes identically in this model due to the quenched random interactions. The two-time self-correlation satisfies scaling with  $R \sim t^{1/z(T)}$  cannot be simply associated to a typical radius of equilibrated domains. The question as to whether the scaling function  $f$  is super-universal is not well posed since the  $T$ -dependent power  $1/z(T)$  can be absorbed in  $f$ . The four-point correlation allows for the definition of a two-time growing length scale  $\xi$  that behaves qualitatively as in Eq. (10). In Fig. 7 we present  $\xi(t, t_w)$  for the 3d EA. Its behaviour is very similar to the one of the RFIM exposed previously, but we would like to stress the fact that this quantity reaches much lower values in the 3d EA case (around  $2a$ ) than in the RFIM (around  $15a$ ). Figure 7 (c) demonstrates that the superscaling property

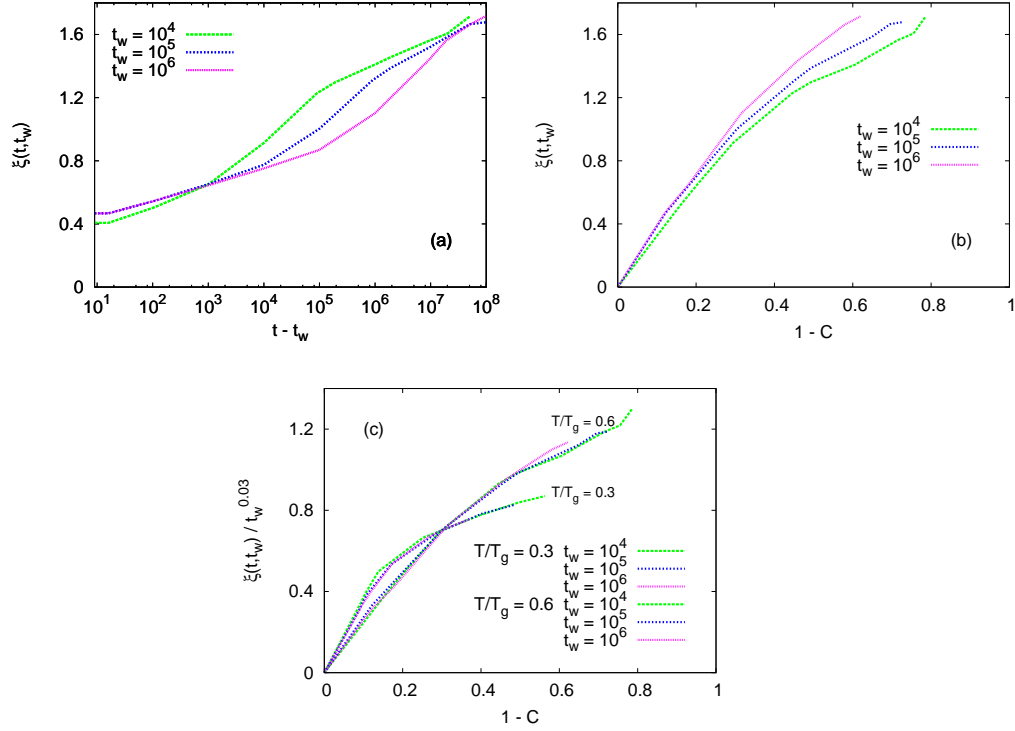


**Figure 7.** Study of the two-time correlation length in the 3d EA model. (a)  $\xi$  as a function of time-delay  $t - t_w$  for several  $t_w$ 's given in the key at  $T/T_g = 0.6$ . (b) Evolution of  $\xi$  with the global correlation in a parametric plot at  $T/T_g = 0.6$ . (c) Test of the scaling hypothesis  $\xi(t, t_w) = R(t_w) g(C)$  with  $R(t) \propto t^{0.03}$  at  $T/T_g = 0.3$  and  $T/T_g = 0.6$ .

does not hold in the 3d EA model. We used  $R(t) \propto t^{0.03}$  for both temperatures and the resulting  $g(C)$  curves are significantly different. It is important to remark that no  $T$ -dependent power-law in  $R$  would make the two curves collapse. Turning back to the scaling of the two-time correlation and fixing the power law,  $C \propto f[(t/t_w)^{0.03}]$  one finds  $f(x) \sim x^{-4.5}$  (at  $T/T_g \sim 0.6$ ) a much faster decaying power than in the RFIM. Note that previous estimates of the dynamic exponent using the one-time replica overlap [12, 13] yield  $1/z(T = 0.3T_g) \approx 0.045$  a slightly larger value; the reason for the discrepancy could be traced to the lack of accuracy in the determination of  $\xi$  and then  $R$ .

### 3.3. Colloidal glasses

The structure factor of colloidal suspensions and Lennard-Jones mixtures are obviously very different from the one of a sample undergoing ferromagnetic ordering. Still, two-time self-correlations satisfy scaling with  $R(t) \propto t^{1/z}$  although a clear interpretation of  $R$  is not available.

Castillo and Parsaeian studied  $\xi$  in a Lennard-Jones mixture of particles undergoing a glassy arrest. One notices that, at short time delays ( $t - t_w \sim 10$  molecular dynamic units),  $\xi$  is monotonic with respect to  $t - t_w$  and  $t_w$  in this system, while one needs to

reach much longer time delays (and indeed go beyond the simulation window) in the 3d EA and RFIM cases [*cfr.* Figs. 5 (a) and 7 (a) to the first panel in Fig. 2 in [17]]. A form like (10) describes  $\xi$  in this case too with  $R(t) \sim t^{1/z}$  and  $1/z \sim 0.1$ .

The two-time correlation length of colloidal suspensions was analysed in [18] using a mapping to a spin problem. The data for  $\xi$  remains, though, quite noisy and although a similar trend in time emerges the precise functional form is hard to extract.

### 3.4. Summary

In short, the macroscopic correlations in all these systems admit the same dynamic scaling analysis although there is no clear interpretation of  $R$  as a domain size in the case of the 3d EA and colloidal suspensions.

## 4. Fluctuations

An approach apt to describe problems with and without quenched randomness focuses on thermally induced fluctuations [19]. The local dynamics can then be examined by studying two-time spin-spin functions which, instead of being spatially averaged over the whole bulk, are only averaged over a coarse-graining cell with volume  $V_r = (2l)^3$  centered at some site  $r$  [16]:

$$C_r(t, t_w) \equiv \frac{1}{V_r} \sum_{\vec{r}_i \in V_r} s_i(t) s_i(t_w). \quad (13)$$

One can then characterize the fluctuations by studying their probability distribution function (pdf)  $\rho(C_r; t, t_w, l, L, T, H)$  with mean value  $C(t, t_w)$ .

In general, the variation of  $\rho(C_r)$  with the size of the coarse-graining boxes is as follows. For  $l < R$  the pdf is peaked around  $q_{\text{EA}}$  and has a fat tail towards small values of  $C_r$  including negative ones. Indeed, well in the coarsening regime, most of the small coarse-grained cells fall inside domains and one then expects to find mostly a thermal equilibrium distribution – apart from the tail. For larger values of  $l$  such as  $l \simeq R$ , a second peak close to  $C$  appears and the one at  $q_{\text{EA}}$  progressively diminishes in height. For still larger values of  $l$ , the peak at  $q_{\text{EA}}$  disappears and a single peak centered at  $C$  (the mean value of the distribution) takes all the pdf weight.

At fixed temperature and field, the pdf  $\rho(C_r; t, t_w, l, L)$  in the RFIM depends on four parameters, two times  $t$  and  $t_w$  and two lengths  $l$  and  $L$ . In the *aging* regime the dependence on  $t$  and  $t_w$  can be replaced by a dependence on  $C(t, t_w)$  and  $\xi(t, t_w)$ , the former being the global correlation and the latter the two-time dependent correlation length. Indeed,  $C(t, t_w)$  is a monotonic function on the two times [*cfr.* Fig. 3 (a)] and  $\xi$  is a growing function of  $t$  (*cfr.* Fig. 1), thus allowing for the inversion  $(t, t_w) \rightarrow (C, \xi)$ . Note that we do not need to enter the aging, coarsening regime to propose this form. One can now make the natural scaling assumption that the pdfs depend on  $\xi$ , the coarse-graining length  $l$ , and the system linear size  $L$  through the ratios  $l/\xi$  and  $l/L$ . In the

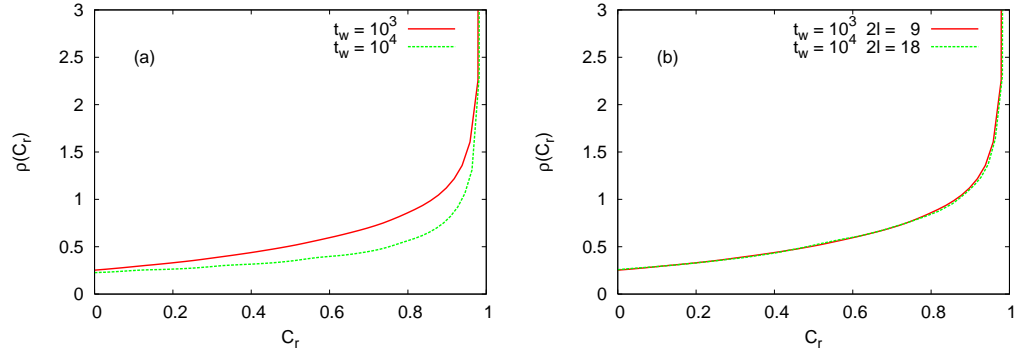


**Figure 8.** Pdf of local two-time functions  $C_r$  in the RFIM at  $T = 1$  and  $H = 1$ . The waiting-times are given in the key and time  $t$  is chosen such that  $C(t, t_w) = 0.6$ . (a)  $C_r$  is coarse-grained on boxes of linear size  $l = 9$ . (b)  $C_r$  is coarse-grained on boxes with variable length  $l$  so as to keep  $l/\xi(t, t_w) \simeq 0.7$  constant. The collapse is much improved with respect to panel (a).

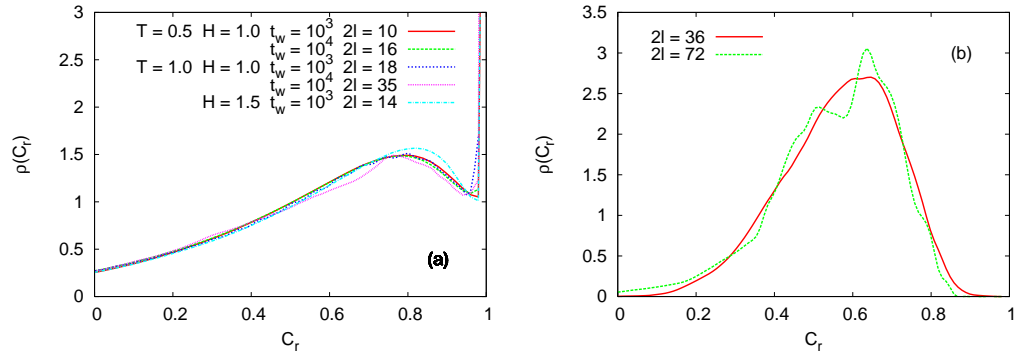


**Figure 9.** Test of the scaling and super-scaling hypothesis. The two pairs of  $t$  and  $t_w$  are the same as in Fig. 8 and  $C = 0.6$  as well. (a)  $l/\xi \simeq 1.4$ . (b)  $l/\xi \simeq 2.9$ .

end, the pdfs characterizing the heterogeneous aging of the system read

$$\rho(C_r; C(t, t_w), l/\xi(t, t_w), l/L). \quad (14)$$

We numerically test this proposal by assuming that the thermodynamic limit applies and the last scaling ratio vanishes identically. Figure 8 (a) shows the pdfs at two pairs of times  $t$  and  $t_w$  such that the global correlation  $C(t, t_w)$  is the same, and  $l = 9$ . It is clear that the two distributions are different. In panel (b) we further choose  $l$  so that  $l/\xi \simeq 0.7$  is also fixed. The two distributions now collapse as expected from the scaling hypothesis Eq. (14). Note that another peak at  $C = -1$  exists, though with a lower weight. Figure 9 (a) and (b) show the scaling for  $l/\xi \simeq 1.4$  and  $l/\xi \simeq 2.9$ , respectively. While the collapse is still good in the case of panel (a), it is not satisfactory in panel (b). Indeed, this plot suffers from the fact that the thermodynamic limit is far from being reached ( $l/L \sim 0.15$  is not so small).

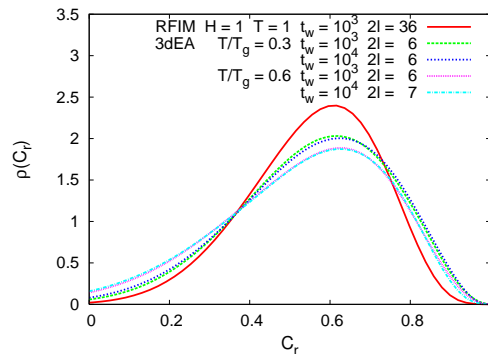


**Figure 10.** Pdf of local correlations in the 3d EA model at  $T/T_g = 0.3$  and  $T/T_g = 0.6$ , for two waiting-times  $t_w$  such that  $C = 0.6$  and  $l/\xi = 2.9$ . The solid line (red) displays the super-universal pdf in the RFIM.

In Fig. 9 (a) we used several values of  $T$  and  $H$  and we found that all pdfs collapse on the same master curve. We conclude that as long as coarse-graining lengths are not too close to the system size, the pdf of local correlation satisfy the scaling (14) with a scaling function that is super-universal.

Let us now compare the forms of the pdfs in the RFIM and 3d EA model. In the RFIM the peak at  $q_{EA}$  is visible until  $l/\xi \simeq 2$ . Given that in this model  $\xi$  is quickly rather large ( $\xi$  reaches  $15a$  in the simulation time-window) one has a relatively large interval of  $l$  for which the peak at  $q_{EA}$  can be easily seen. Instead, in the 3d EA the two-time correlation length grows very slowly and reaches only  $\xi \sim 2a$  in similar times, meaning that the peak at  $q_{EA}$  is hardly visible as soon as one coarse-grains the two-time observables [14].

Figure 10 demonstrates that the pdf of local correlations is not super-universal with respect to  $T$  in the 3d EA model, and compares the functional form at two temperatures,  $T/T_g = 0.3$  and  $T/T_g = 0.6$ , with the one in the RFIM. The global correlation,  $C$ , and the ratio of coarse-graining to correlation lengths,  $l/\xi$ , are the same in all curves. Although qualitatively similar, the pdf in the RFIM and 3d EA models are different, with the RFIM one being more centered around the global value.

The study of Lennard-Jones mixtures in [23] used a constant coarse-graining length and the pdfs of local correlations at constant  $C$  showed a slow drift that should be cured by taking into account the variation of  $\xi$ . In colloidal suspensions the scaling form (14) is well satisfied [18]. In the context of coarsening phenomena these pdfs are to be compared to the ones calculated for the  $O(N)$  model in its large  $N$  limit [20].

## 5. Conclusion

We performed an extensive analysis of the dynamics of the RFIM in its coarsening regime. We showed that the equal-time correlation functions, global two-time correlation functions, and the four point correlation functions obey scaling and super-universality relations in the aging regime. The scaling relations, by means of the typical growing

length,  $R \propto \ln t/\tau$ , reveal a non-trivial time-invariance for these statistical objects. Super-universality encodes the irrelevance of quenched randomness and temperature on the scaling functions and it is demonstrated by the fact that they are the same as for the pure Ising case.

In the 3d EA, similar scaling forms were found for global two-time correlations and four-point correlations [14]. The function  $R(t)$  could be associated to a domain radius though a clearcut confirmation of this is lacking. On the contrary, the results of recent large scale simulations have been interpreted as evidence for an SK-like dynamic scenario [15]. The one-time function playing the role of the domain radius is a very weak power law,  $t^{0.03}$  at  $T/T_g \sim 0.3 - 0.6$ , and, in consequence, the two-time correlation length reaches much shorter values than in the RFIM in equivalent simulation times. Super-universality (with respect to temperature) does not apply in this case.

A similar scenario applies to the Lennard-Jones mixtures [23] and colloidal suspensions [18]. The two-time correlation length remains also very short in accessible numerical and experimental times.

In all these systems the analysis of local fluctuations of two-time functions leads to scaling of their probability distribution functions. In the RFIM these also verify super-scaling with respect to  $T$  and  $H$ . In the 3d EA they do not. The intriguing possibility of a kind of super-scaling in colloidal suspensions (with respect to concentration) has been signaled in [18] and deserves a more careful study.

We conclude that all these systems, with *a priori* very different microscopic dynamic processes admit a similar dynamic scaling description of their macroscopic and mesoscopic out of equilibrium evolution.

## Acknowledgments

We thank L. D. C. Jaubert and A. Sicilia for very useful discussions and T. Malakis and V. Martín-Mayor for helpful correspondence. LFC is a member of Institut Universitaire de France.

- [1] A. J. Bray, Adv. Phys. **43**, 357 (1994).
- [2] S. Puri, Phase Transitions **77**, 407 (2004).
- [3] T. Nattermann and J. Villain, Phase Transitions **11**, 5 (1988). T. Nattermann and P. Rujan, Int. J. Mod. Phys. **3**, 1597 (1989). T. Nattermann, cond-mat/9705295 in *Spin glasses and random fields*, A. P. Young ed. (World Scientific, Singapore, 1997).
- [4] R. Paul, G. Schehr, and H. Rieger, Phys. Rev. E **75**, 030104(R) (2007). R. Paul, S. Puri, and H. Rieger Phys. Rev. E **71**, 061109 (2005) F. Baumann, M. Henkel, and M. Pleimling *Phase-ordering kinetics of two-dimensional disordered Ising models*, arXiv:0709.3228. H. Hinrichsen, *Dynamical response function of the disordered kinetic Ising model* arXiv:0711.2421.
- [5] D. S. Fisher and D. A. Huse, Phys. Rev. B **38**, 373 (1988).
- [6] M. Rao and A. Chakrabarti, Phys. Rev. Lett. **71**, 3501 (1993).



- [7] S. Puri and N. Parekh, J. Phys. A **26**, 2777 (1993). A. J. Bray and K. Humayun, J. Phys. A **24**, L1185 (1991).
- [8] A. Sicilia, J. J. Arenzon, A. J. Bray and L. F. Cugliandolo, EPL **82**, 10001 (2008).
- [9] L. F. Cugliandolo and J. Kurchan, J. Phys. A **27** 5749 (1994).
- [10] A. Baldassarri, L. F. Cugliandolo, J. Kurchan and G. Parisi, J. Phys. A **28** 1831 (1995).
- [11] H. Rieger, J. Phys. A **26**, L615 (1993). T. Komori, H. Takayama, and H. Yoshino, J. Phys. Soc. Jpn. **68**, 3387 (1999), *ibid* **69**, 1192 (1999), **69** Suppl. A 228 (2000). M. Picco, F. Ricci-Tersenghi and F. Ritort, Eur. Phys. J. B **21**, 211 (2001).
- [12] J. Kisker, L. Santen, M. Schreckenberg, and H. Rieger, Phys. Rev. B **53** 6418 (1996).
- [13] E. Marinari, G. Parisi, F. Ricci-Tersenghi, and J. J. Ruiz-Lorenzo, J. Phys. A **33**, 2373 (2000).
- [14] L. D. C. Jaubert, C. Chamon, L. F. Cugliandolo and M. Picco J. Stat. Mech., P05001 (2007).
- [15] F. Belletti, M. Cotallo, A. Cruz, L.A. Fernandez, A. Gordillo-Guerrero, M. Guidetti, A. Maiorano, F. Mantovani, E. Marinari, V. Martin-Mayor, A. Munoz Sudupe, D. Navarro, G. Parisi, S. Perez-Gaviro, J.J. Ruiz-Lorenzo, S.F. Schifano, D. Sciretti, A. Tarancon, R. Tripiccion, J.L. Velasco, D. Yllanes (the Janus collaboration), *Simulating an Ising spin-glass for 0.1 seconds with Janus*, arXiv:0804.1471.
- [16] H. E. Castillo, C. Chamon, L. F. Cugliandolo, M. P. Kennett, Phys. Rev. Lett. **88**, 237201 (2002). H. E. Castillo, C. Chamon, L. F. Cugliandolo, J. L. Iguain, M. P. Kennett, Phys. Rev. B **68**, 134442 (2003).
- [17] A. Parsaeian and H. E. Castillo, *Growth of spatial correlations in the aging of a simple structural glass*, arXiv:cond-mat/0610789.
- [18] C. Chamon, L. F. Cugliandolo, G. Fabricius, J. L. Iguain and E. R. Weeks, arXiv:0802.3297
- [19] C. Chamon and L. F. Cugliandolo, J. Stat. Mech. (2007) P07022.
- [20] C. Chamon, L. F. Cugliandolo and H. Yoshino, J. Stat. Mech (2006) P01006.
- [21] P. Mayer, H. Bissig, L. Berthier, L. Cipelletti, J. P. Garrahan, P. Sollich and V. Trappe, Phys. Rev. Lett. **93**, 115701 (2004); P. Mayer, P. Sollich, L. Berthier and J. P. Garrahan, J. Stat. Mech. (2005) P05002.
- [22] C. Chamon, P. Charbonneau, L. F. Cugliandolo, D. R. Reichman and M. Sellitto, Journal of Chemical Physics **121**, 10120 (2004).
- [23] A. Parsaeian and H. E. Castillo, Nature Phys. **3**, 26 (2007).
- [24] Y. Imry and S. K. Ma, Phys. Rev. Lett. **35**, 1399 (1975).
- [25] D. P. Belanger, Phase Transitions **11**, 53 (1988). D. P. Belanger in *Spin glasses and random fields*, A. P. Young ed. (World Scientific, Singapore, 1997).
- [26] F. Alberici-Kious, J-P Bouchaud, L. F. Cugliandolo, P. Doussineau and A. Levelut, Phys. Rev. Lett. **81**, 4987 (1998); Phys. Rev. B **62**, 14766 (2000).
- [27] J. Z. Imbrie, Phys. Rev. Lett. **53**, 1747 (1984).
- [28] J. Brimont and A. Kupiainen, Phys. Rev. Lett. **59**, 1829 (1987).
- [29] A. P. Young and M. Nauenberg, Phys. Rev. Lett. **54**, 2429 (1985).
- [30] H. Rieger, Phys. Rev. B **52**, 6659 (1995).
- [31] A. A. Middleton and D. S. Fisher, Phys. Rev. B **65**, 134411 (2002).
- [32] M. Mézard and A. P. Young, Europhys. Lett. **18**, 653 (1992). M. Mézard and R. Monasson, Phys. Rev. B **50**, 7199 (1994).
- [33] M. R. Swift, A. J. Bray, A. Maritan, M. Cieplak and J. R. Banavar, Europhys. Lett. **38**, 273 (1997).
- [34] A. Malakis and N. G. Fytas, Eur. Phys. J. B **51**, 257 (2006). A. Malakis and N. G. Fytas, Eur. Phys. J. B **61**, 111 (2008). N. G. Fytas, A. Malakis, and K. Eftaxias, J. Stat. Mech. (2008) P03015.
- [35] H. G. Ballesteros, A. Cruz, L. A. Fernandez, V. Martín-Mayor, J. Pech, J. J. Ruiz-

- Lorenzo, A. Tarancon, P. Tellez, C. L. Ullod, C. Ungil, Phys. Rev. B **62** 14237 (2000).
- [36] K. H. Fischer and J. A. Hertz *Spin glasses*, (Cambridge Univ. Press. 1991).
  - [37] A. B. Bortz, M. H. Kalos and J. L. Lebowitz, J. Comp. Phys. **17**, 10 (1975).
  - [38] J. Dall and P. Sibani, Comp. Phys. Comm. **141**, 260 (2001).
  - [39] M. A. Novotny, Ann. Rev. Comp. Phys. **IX**, editor D. Stauffer (World Scientific, Singapore, 2001), p.153.
  - [40] A way to check whether a spin-glass model gets close to equilibration is to follow the evolution of spin replicas with the same quenched randomness and testing when the overlap distribution develops a non-trivial structure. Some papers explaining and using this technique are [10], N. D. Mackenzie and A. P. Young, Phys. Rev. Lett. **49**, 301 (1982); K. Binder and A. P. Young, Rev. Mod. Phys. **58**, 801 (1986).
  - [41] Note that some coarsening problems have a distribution of domain radii with long-tails, see J. J. Arenzon, A. J. Bray, L. F. Cugliandolo and A. Sicilia, Phys. Rev. Lett. **98**, 145701 (2007) and [42].
  - [42] A. Sicilia, J. J. Arenzon, A. J. Bray and L. F. Cugliandolo, Phys. Rev. E **76**, 061116 (2007).
  - [43] J. Villain, Phys. Rev. Lett. **52**, 1543 (1984). J. Villain, J. Physique Lett. (France) **43**, L551 (1982).
  - [44] G. Grinstein and S. K. Ma, Phys. Rev. Lett. **49**, 685 (1982).
  - [45] G. Grinstein and J. F. Fernandez, Phys. Rev. Lett. **29**, 6387 (1984). J. F. Fernández, Europhys. Lett. **5**, 129 (1988).
  - [46] R. Bruinsma and G. Aeppli, Phys. Rev. Lett. **52**, 1547 (1984).
  - [47] S. R. Anderson, Phys. Rev. B **36**, 8435 (1987).
  - [48] E. Oguz, J. Phys. A **27**, 2985 (1994).
  - [49] N. Lacevic, F. W. Starr, T. B. Schroder, V. N. Novikov and S. C. Glotzer, Phys. Rev. E **66**, 030101 (R) (2002).